

Heterogeneous photocatalytic degradation of anthraquinone dye Reactive Blue 19: optimization, comparison between processes and identification of intermediate products

Miljana D Radović Vučić¹, Jelena Z Mitrović¹, Miloš M Kostić¹, Nena D Velinov¹, Slobodan M Najdanović¹, Danijela V Bojić¹ and Aleksandar Lj. Bojić¹

¹Department of Chemistry, Faculty of Science and Mathematics, The University of Niš, Višegradska 33, 18000 Niš, Serbia

Treatment of textile wastewater using heterogeneous photocatalysis began in the the last decade and attracted the attention of researchers due to its versatile application. The variety of applications of TiO₂ as a photocatalyst was due to its numerous positive properties, such as low operating temperature, biologically inert nature, low energy consumption, water insolubility, availability and photoactivity, low toxicity, high chemical stability, suitable flat band potential, narrow bandgap and the fact that it is environmentally benign. Heterogeneous UV-TiO₂ photocatalysis is capable of removing organic pollutants from textile wastewater; this has been widely studied, with the technology also having been commercialized in many developing countries. Decolorization of anthraquinone dye Reactive Blue 19 (RB 19) by heterogeneous advanced oxidation processes TiO₂/UV/H₂O₂, TiO₂/UV/KBrO₃ and TiO₂/UV/(NH₄)₂S₂O₈ was studied under different conditions and in the presence of electron acceptors such as hydrogen peroxide (H₂O₂), potassium bromate (KBrO₃) and ammonium persulphate ((NH₄)₂S₂O₈). Decolorization was very fast for all three processes, and complete dye decolorization was achieved in 10 min. The effect of various ions (Cl⁻, SO₄²⁻ and HCO₃⁻) on RB 19 decolorization was also studied. The optimal condition for the decolorization of the dye were determined to be: TiO₂ concentration 1 g·dm⁻³, electron acceptor concentration 30.0 mmol·dm⁻³, dye concentration 50.0 mg·dm⁻³, UV intensity 1 950 μW·cm⁻², at temperature 25 ± 0.5°C. In addition, experiments were performed and compared in three different matrices. In the surface water and dye bath effluent water, the removal efficiency for RB 19 was lower than that achieved in the deionized water because of the interference of complex constituents in the surface water and effluent. LC-MS analysis was carried out and the detected intermediates were compared with the previously published data for anthraquinone dyes.

CORRESPONDENCE

Miljana D Radović Vučić

EMAIL

mimaradovic@gmail.com

DATES

Received: 12 December 2018

Accepted: 30 March 2020

KEYWORDS

anthraquinone dye
electron acceptors
photocatalysis
Reactive Blue 19
titanium dioxide

COPYRIGHT

© The Author(s)

Published under a Creative

Commons Attribution 4.0

International Licence (CC BY 4.0)

INTRODUCTION

Textile industries play a vital role in the economic development of many developing countries and therefore also in increasing the gross domestic products of these countries (Masum, 2016). These industries use different raw materials, such as cotton, synthetic and woollen fibres, and chemicals including dyes. Approximately 10 000 different synthetic dyes are available in the market and worldwide annual production of these dyes is over 700 000 t. Nearly 200 000 t of synthetic dyes are lost into the environment because of the inefficient dyeing process used in textile industries. According to World Bank estimates, about 17–20% of industrial wastewater is generated from textile dyeing and finishing treatments (Holkar et al., 2016; Hossain et al., 2018; Ribeiro et al., 2017).

Thus, though the textile industry provides significant economic benefits, it also faces the environmental and social impacts associated with the generation of toxic wastewaters from its processing operations, such as de-sizing, sizing, scouring, bleaching, mercerizing, dyeing, printing, finishing and other processes (Masum, 2016; Miguel et al., 2002; Ledakowicz et al., 2001; Punzi et al., 2015). In order to meet the colour requirement, reactive and azo dyes are highly water-soluble and therefore around 10–20% of the used dye is washed out with water as effluents which are hazardous (carcinogenic or mutagenic) and toxic to the environment (Ganesh et al., 1994; Weber and Adams, 1995; Zhang et al., 1998).

Various treatment technologies have been developed for the textile wastewater, namely, physical, chemical and biological treatment (Ganesh et al., 1994; Weber and Adams, 1995). In recent years much attention has been given to advanced oxidation processes (AOPs). AOPs include a number of approaches, such as UV photolysis, Fenton process, photo-Fenton process, electro-Fenton process, photoelectro-Fenton, ozonation process, sonolysis, catalytic and radiation-induced biodegradation, etc. (Mohej et al., 2003; Muruganandham and Swaminathan, 2004a; Flox et al., 2006; Chen et al., 2002; Daneshvar and Khataee, 2006; Shu and Chang, 2005; Brillas et al., 2000; Rosenfeldt et al., 2006; Daneshvar et al., 2003; Daneshvar et al., 2005a; Piera et al., 2000; Daneshvar et al., 2007; Elmorsi et al., 2010; Tehrani-Bagha et al., 2010; Wang et al., 2008; Rauf et al., 2010; Ayed et al., 2010; Chen et al., 2008). Photocatalysis relies on the formation and utilization of OH• radicals and lead to the breakdown of contaminants into water, CO₂ and less harmful products. Various semiconductors such as TiO₂, ZnO, Fe₂O₃, CdS, ZnS and V₂O₅ can be used for photocatalysis because of their suitable bandgap energy.

Heterogeneous photocatalysis is based on the reactive properties of photogenerated electron-hole carriers. When a semiconducting material is illuminated by light with an appropriate wavelength, electron-hole pairs are generated. The photogenerated hole, an electron donor, can react with the adsorbed water and hydroxide ions (OH^-) to form hydroxyl radicals ($\text{OH}\cdot$), whereas the photogenerated electron can react with oxygen to form superoxide radical ion ($\text{O}_2\cdot^-$). Both $\text{OH}\cdot$, $\text{O}_2\cdot^-$ and the photogenerated hole are capable of oxidizing a host of organic and inorganic compounds (Linsebigler and Yates, 1995; Fujishima et al., 2000; Fox and Dulay, 1993). It has been demonstrated that TiO_2 is one of the most significant inorganic photocatalytic materials (Subramanian et al., 2001), in particular the commercial Degussa P25.

Semiconductor TiO_2 -based photocatalysis has received much attention because of its properties such as non-toxicity, chemical and biological stability, low cost and higher photocatalytic activity. However, for the technical and commercial feasibility of the process, extensive investigations are needed to overcome some problems with TiO_2 -based photocatalysts (Sharotri and Sud, 2017).

One of the major disadvantages of heterogeneous photocatalysis is the recombination of the photo-generated electron (e_{cb}^-) and hole (h_{vb}^+). This step decreases the quantum yield and causes energy wasting. These could be overcome by using electron acceptors or hole scavengers. The addition of the electron acceptor, such as KBrO_3 , H_2O_2 and $(\text{NH}_4)_2\text{S}_2\text{O}_8$ enhanced the degradation rate by (i) preventing the electron-hole recombination by accepting the conduction band electron; (ii) increasing the hydroxyl radical concentration; and (iii) generating other oxidizing species ($\text{SO}_4\cdot^-$) to improve the efficiency of intermediate compounds (Wei et al., 2009).

The objective of the present study was to evaluate the effectiveness of heterogeneous advanced oxidation processes $\text{TiO}_2/\text{UV}/\text{KBrO}_3$, $\text{TiO}_2/\text{UV}/\text{H}_2\text{O}_2$ and $\text{TiO}_2/\text{UV}/(\text{NH}_4)_2\text{S}_2\text{O}_8$ at degrading the anthraquinone dye Reactive Blue 19 (RB 19). For all three processes, the influence of background ions Cl^- , SO_4^{2-} and HCO_3^- , which can compete with the target contaminant for reaction with radicals and holes, was examined. The effect of these ions has not been reported in the literature. Therefore, the influence of the aqueous matrix should also be considered when applying $\text{TiO}_2/\text{UV}/\text{KBrO}_3$, $\text{TiO}_2/\text{UV}/\text{H}_2\text{O}_2$ and $\text{TiO}_2/\text{UV}/(\text{NH}_4)_2\text{S}_2\text{O}_8$ in practice. For this reason, experiments were performed in three different matrixes (laboratory deionized water, surface water collected from the local Nišava River and dyebath effluent water from a local cotton dyeing facility).

Most investigators have provided information on dyes removal during the degradation process and not much information has been provided about the degradation pathway or intermediate compound formation by heterogeneous advanced oxidation processes $\text{TiO}_2/\text{UV}/\text{KBrO}_3$, $\text{TiO}_2/\text{UV}/\text{H}_2\text{O}_2$ and $\text{TiO}_2/\text{UV}/(\text{NH}_4)_2\text{S}_2\text{O}_8$. Hence in the present study, an attempt was made to identify the intermediate compound formed during the dye photocatalytic degradation by using LC-MS analysis.

MATERIALS AND METHODS

Reagents

The anthraquinone reactive dye C.I. Reactive Blue 19 (RB 19) ($\text{Mw} = 626.55 \text{ g}\cdot\text{mol}^{-1}$) was obtained from Sigma-Aldrich (USA) and used without any purification. The hydrogen peroxide (H_2O_2) solution (30.0%), potassium bromate (KBrO_3) and ammonium persulfate ($(\text{NH}_4)_2\text{S}_2\text{O}_8$) were of analytical grade and purchased from Merck (Germany). Commercially produced titanium dioxide (TiO_2 -P25) was used in all experiments. TiO_2 -P25

was received from Degussa (Frankfurt, Germany). TiO_2 -P25 contains anatase 80.0 and rutile 20.0 with mean particle size of 30.0 nm and BET surface area of $50.0 \text{ m}^2\cdot\text{g}^{-1}$.

Photoreactor

Photochemical experiments were carried out in a batch photoreactor handmade in our laboratory (Mitrovic et al., 2012). The UV lamps were turned on 10 min before performing each experiment. The intensity of UV radiation was measured by a UV radiometer Solarmeter model 8.0 UVC (Solartech, USA). The total UV intensity was controlled by turning on different numbers of UV lamps and the maximum intensity was $1\,950 \mu\text{W}\cdot\text{cm}^{-2}$ (with all ten UV lamps on) at a distance of 220 mm from the working solution surface.

Procedures

A stock solution of RB 19 was prepared by dissolving 1.0 g dye in $1\,000.0 \text{ cm}^3$ of deionized water. Working solutions were freshly prepared before irradiation, by diluting the stock to the desired concentration with deionized water. The pH of the solutions was adjusted by addition of NaOH or HCl ($0.1/0.01 \text{ mol}\cdot\text{dm}^{-3}$) with pH/ISE meter (Orion Star A214, Thermo scientific, USA). The suspensions of dye and TiO_2 were magnetically stirred in the dark for 30 min to attain adsorption-desorption equilibrium between dye and TiO_2 , and the dye solutions were then treated in the UV reactor.

During irradiation, the solution was magnetically stirred (Are, Velp Scientifica, Italy) at a constant rate, and temperature was maintained at $25 \pm 0.5^\circ\text{C}$ by thermostating. At required time intervals, 4.0 cm^3 of samples were withdrawn, centrifuged ($3\,000 \text{ r}\cdot\text{min}^{-1}$, 15 min) and filtered through a $0.20 \mu\text{m}$ regenerated cellulose membrane filter (Agilent Technologies, Germany) to separate the catalyst. Absorbance at 592 nm was measured using a UV-vis spectrophotometer Shimadzu UV-1800 PC (Shimadzu, Japan) to determine the degree of decolorization of the solution. The removal (%) of RB 19 dye was calculated as:

$$\text{Removal}(\%) = \left[1 - \frac{c_t}{c_0} \right] \times 100 \quad (1)$$

where c_0 and c_t are the concentration values of the dye solution before and after UV irradiation, respectively.

Identifying the degradation product of the RB 19 solution was carried out by LC-MS system. After treatment, the samples of RB 19 were processed using LCQ Fleet mass spectrometer (Thermo Fisher Scientific, USA) with orthogonal electrospray (ESI) source and ion trap (IT) as an analyser. The LCQ Fleet mass spectrometer was linked to the HPLC system (Ultimate 3000, Thermo Fisher Scientific, USA). Thermo Scientific column Dionex Hipersil GOLD C18 was used for separation in a liquid chromatograph. The samples of anthraquinone dye RB 19 were analysed in a negative mode of the mass spectrometer.

To ensure the accuracy, reliability, and reproducibility of the collected data, all experiments were carried out in triplicate, and mean values are recorded. OriginPro 2016 (OriginLab Corporation) software was used for statistical analysis and calculation of the data.

RESULTS AND DISCUSSION

Influence of experimental parameters on removal efficiency of RB 19

The preliminary experiments were carried out in order to investigate the effect of UV radiation only, TiO_2 without UV

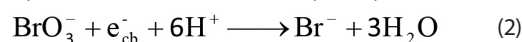
radiation, electron acceptors (KBrO_3 , H_2O_2 and $(\text{NH}_4)_2\text{S}_2\text{O}_8$) without UV radiation and UV irradiation in the presence of TiO_2 and electron acceptors. The solution of RB 19 dye (initial dye concentration was $50.0 \text{ mg}\cdot\text{dm}^{-3}$) was irradiated for 180 min to examine the effect of UV light radiation alone, and there was no observable decrease in residual dye concentration. This indicated that the direct photolysis of RB 19 dye by UV irradiation was slow. Experiments with only electron acceptors were done for 180 min in the dark. The dye removal efficiency, in that case, was also negligible. No decolorization was observed for the dye solution with TiO_2 without UV radiation. But if electron acceptors are applied in combination with UV radiation and TiO_2 , residual dye concentration rapidly decreases (Fig. 1). Complete decolorization was obtained in less than 15 min, with an initial dye concentration of $50.0 \text{ mg}\cdot\text{dm}^{-3}$ in the presence of $1.0 \text{ g}\cdot\text{dm}^{-3}$ TiO_2 and $30.0 \text{ mmol}\cdot\text{dm}^{-3}$ electron acceptors and under $1950 \mu\text{W}\cdot\text{cm}^{-2}$ light intensity.

Titanium dioxide has drawn much attention from the industry as a good candidate for a large band-gap semiconducting oxide for photodecomposition processes in pollutant treatment, because of its favourable physical/chemical properties, low cost, ease of availability, and high stability (Wang et al., 2013; Yang et al., 2013; Xu et al., 2013; Cetinkaya et al., 2013). Numerous studies in the literature show that TiO_2 and other catalysts remain unchanged after the photocatalytic process, confirming their stability even after several cycles of use. (Wan et al., 2012; Li and Wu, 2017; Zhu et al., 2011). Because of all the abovementioned factors, TiO_2 was selected as a photocatalyst in the processes examined in this manuscript. The process optimization for the best dye removal efficiency is presented below.

Effect of electron acceptors

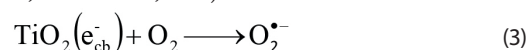
BrO_3^- ion is an efficient electron acceptor and is used to enhance photocatalytic decolorization rate (Poulios and Tsachpinis, 1999; Gratzel et al., 1990; Sanchez et al., 1998). The effect of the addition of KBrO_3 (10.0 – $100.0 \text{ mmol}\cdot\text{dm}^{-3}$) on removal efficiency of RB 19 is shown in Fig. 2. It can be seen that adding a small amount of KBrO_3 , from 10.0 to $30.0 \text{ mmol}\cdot\text{dm}^{-3}$, increases the decolorization from 88.62% to 96.38% during the time period of 10 min. The enhancement of the removal efficiency is due to the reaction between BrO_3^- ion and conduction band electron (Eq. 2) (Wei

et al., 2009; Muneera and Bahnemann, 2002; San et al. 2001)

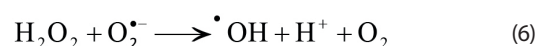


With the further increase in KBrO_3 concentration from 30.0 to $100.0 \text{ mmol}\cdot\text{dm}^{-3}$ the removal efficiency is almost constant. This is due to the adsorption effect of Br^- ions on the TiO_2 surface, which affects the catalytic activity of TiO_2 (San et al., 2001). So the optimum concentration of bromate ion is $30.0 \text{ mmol}\cdot\text{dm}^{-3}$ for photocatalytic decolorization of RB 19.

The photocatalytic decolorization of dye occurs on the surface of TiO_2 , and O_2 and H_2O_2 are necessary for photocatalytic decolorization (Vesely et al., 1991; Chen and Liu, 2007; Dionysiou et al., 2000; Houas et al., 2001):



H_2O_2 may be photolyzed or react with superoxide anion to form hydroxyl radical directly:



The initial concentration of H_2O_2 plays an important role in the $\text{TiO}_2/\text{UV}/\text{H}_2\text{O}_2$ process. The effect of the addition of H_2O_2 (10.0 – $100.0 \text{ mmol}\cdot\text{dm}^{-3}$) on the decolorization of RB 19 is shown in Fig. 2. The addition of H_2O_2 from 10.0 to $30.0 \text{ mmol}\cdot\text{dm}^{-3}$ increases the decolorization from 59.52% to 87.79% at 10 min. A further increase from 30.0 to $100.0 \text{ mmol}\cdot\text{dm}^{-3}$ decreases the removal efficiency to 64.12% within 10 min. A similar observation has been reported for other organic pollutants (Wei et al., 2009; So et al., 2002; Chu and Wong, 2004). The increase in the decolorization is due to the increase in hydroxyl radical concentration by the addition of H_2O_2 . At a high dosage of H_2O_2 the decrease in decolorization is due to the hydroxyl radical scavenging effect of H_2O_2 and recombination of hydroxyl radicals (Daneshvar et al., 2005b; Aleboye et al., 2005):

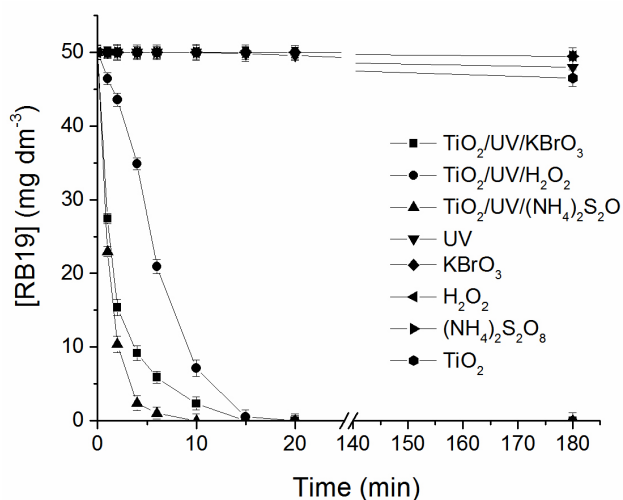


Figure 1. Effect of UV light, TiO_2 , electron acceptors $\text{TiO}_2/\text{UV}/\text{KBrO}_3$, $\text{TiO}_2/\text{UV}/\text{H}_2\text{O}_2$ and $\text{TiO}_2/\text{UV}/(\text{NH}_4)_2\text{S}_2\text{O}_8$ processes on decolorization of RB 19. $[\text{RB19}]_0 = 50.0 \text{ mg}\cdot\text{dm}^{-3}$, $[\text{TiO}_2] = 1.0 \text{ g}\cdot\text{dm}^{-3}$, $[\text{KBrO}_3]_0 = 30.0 \text{ mmol}\cdot\text{dm}^{-3}$, $[\text{H}_2\text{O}_2]_0 = 30.0 \text{ mmol}\cdot\text{dm}^{-3}$, $[(\text{NH}_4)_2\text{S}_2\text{O}_8]_0 = 30.0 \text{ mmol}\cdot\text{dm}^{-3}$, initial pH was 7.0, UV radiation intensity was $1950 \mu\text{W}\cdot\text{cm}^{-2}$, temperature was $25 \pm 0.5^\circ\text{C}$.

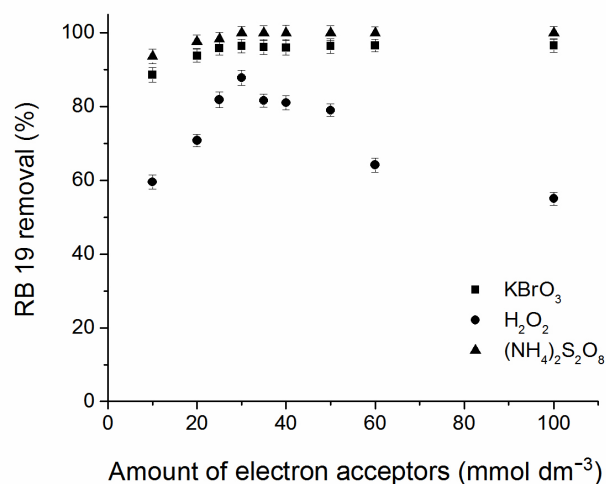
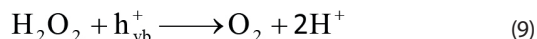


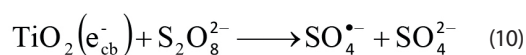
Figure 2. The removal efficiency of RB 19 by $\text{TiO}_2/\text{UV}/\text{KBrO}_3$, $\text{TiO}_2/\text{UV}/\text{H}_2\text{O}_2$ and $\text{TiO}_2/\text{UV}/(\text{NH}_4)_2\text{S}_2\text{O}_8$ processes as a function of initial concentration of electron acceptors. $[\text{RB19}]_0 = 50.0 \text{ mg}\cdot\text{dm}^{-3}$, $[\text{TiO}_2] = 1.0 \text{ g}\cdot\text{dm}^{-3}$, initial pH 7.0, UV radiation intensity was $1950 \mu\text{W}\cdot\text{cm}^{-2}$, temperature was $25.0 \pm 0.5^\circ\text{C}$.



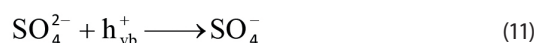
H_2O_2 is also a powerful hole scavenger. In excess, it may react with holes to produce oxygen and protons. In photocatalytic decolorization, the hole directly oxidizes the dye and with water produces a hydroxyl radical. Hence, the removal efficiency for the dye decreases due to the removal of holes (Pichat et al., 1995).



The effect of the addition of $\text{S}_2\text{O}_8^{2-}$ on the photolytic oxidation of RB 19 ($50.0 \text{ mg}\cdot\text{dm}^{-3}$) was investigated by varying the amount of $(\text{NH}_4)_2\text{S}_2\text{O}_8$ from 10.0 to $100.0 \text{ mmol}\cdot\text{dm}^{-3}$. The results are shown in Fig. 2. The addition of $(\text{NH}_4)_2\text{S}_2\text{O}_8$ from 10.0 to $30.0 \text{ mmol}\cdot\text{dm}^{-3}$ increases the removal efficiency from 93.63% to 100.00% within 10 min . These results are in agreement with earlier research (Poulios and Tsachpinis, 1999; Sanchez et al., 1998). With the further increase of $(\text{NH}_4)_2\text{S}_2\text{O}_8$ concentration from 30.0 to $100.0 \text{ mmol}\cdot\text{dm}^{-3}$ the removal efficiency is almost constant. Addition of persulfate to photocatalytic processes enhances the decolorization rate in the following ways:



In the reaction with a photogenerated electron and with a water molecule, the sulfate radical anion $\text{SO}_4^{\bullet-}$ can generate a hydroxyl radical. The sulfate radical anion is a strong oxidant and participates in the decolorization process. At a high dosage of $\text{S}_2\text{O}_8^{2-}$, inhibition of reaction occurs due to the increase in the concentration of the SO_4^{2-} ion. On the surface of the TiO_2 catalyst there is absorption of the SO_4^{2-} ions. Therefore, catalytic activity is reduced. On the other hand, the adsorbed SO_4^{2-} ion also reacted with photogenerated holes (Eq. 11) and hydroxyl radical (Eq. 12).



Effect of initial RB 19 concentration

Pollutant concentration is a very important parameter in wastewater treatment. The effect of initial dye concentration on decolorization was investigated over a range of 10.0 to $100.0 \text{ mg}\cdot\text{dm}^{-3}$. The removal efficiency of RB 19 by $\text{TiO}_2/\text{UV}/\text{KBrO}_3$ after 10 min of treatment is shown in Table 1. The results indicate that while increasing the initial concentration of dye from $10.0 \text{ mg}\cdot\text{dm}^{-3}$ to $100.0 \text{ mg}\cdot\text{dm}^{-3}$ removal efficiency decreased from 100.0% to 82.55% .

Table 1. Effect of initial dye concentration on removal efficiency of RB 19 by $\text{TiO}_2/\text{UV}/\text{KBrO}_3$, $\text{TiO}_2/\text{UV}/\text{H}_2\text{O}_2$ and $\text{TiO}_2/\text{UV}/(\text{NH}_4)_2\text{S}_2\text{O}_8$ processes

Conc. of dye ($\text{mg}\cdot\text{dm}^{-3}$)	Removal efficiency (%)		
	$\text{TiO}_2/\text{UV}/\text{KBrO}_3$	$\text{TiO}_2/\text{UV}/\text{H}_2\text{O}_2$	$\text{TiO}_2/\text{UV}/(\text{NH}_4)_2\text{S}_2\text{O}_8$
10	100.00	95.49	100
20	98.93	93.24	100
30	98.05	89.32	100
40	97.45	85.11	100
50	96.38	87.79	100
60	92.78	65.63	98.78
80	85.07	45.46	95.34
100	82.55	39.14	90.05

The results after 10 min of treatment by $\text{TiO}_2/\text{UV}/\text{H}_2\text{O}_2$ process are shown in Table 1. With the increase in the initial concentration of dye from $10.0 \text{ mg}\cdot\text{dm}^{-3}$ to $100.0 \text{ mg}\cdot\text{dm}^{-3}$, removal efficiency decreases from 95.49% to 39.14% . At high concentrations the penetration of photons entering into the solution decreases, consequently lowering the hydroxyl radical concentration (Ghodbane and Hamdaoui, 2010; Muruganandham and Swaminathan, 2004b; Behnajady et al., 2004; Galindo and Kalt1998). It can be seen that removal efficiency decreased as initial dye concentration increased at the same concentration of $(\text{NH}_4)_2\text{S}_2\text{O}_8$.

Effect of UV radiation intensity

By increasing UV radiation intensity, the efficiency of dye decolorization increases considerably. Based on the obtained results, which are shown in Fig. 3, it can be concluded that removal efficiency of dye increases with the increase in radiation intensity from $730 \text{ }\mu\text{W}\cdot\text{cm}^{-2}$ to $1\,950 \text{ }\mu\text{W}\cdot\text{cm}^{-2}$. The lowest difference within the process efficiency is between the radiation intensity $1\,750 \text{ }\mu\text{W}\cdot\text{cm}^{-2}$ and $1\,950 \text{ }\mu\text{W}\cdot\text{cm}^{-2}$, from which follows that the back lamps in photoreactor have the least contribution to dye decolorization. Results have also shown that the UV intensity tested in the study lies in the linear range and all the photons produced are effectively used (Fig. 3).

The increase in light intensity from $730 \text{ }\mu\text{W}\cdot\text{cm}^{-2}$ to $1\,950 \text{ }\mu\text{W}\cdot\text{cm}^{-2}$ increases the decolorization by $\text{TiO}_2/\text{UV}/\text{H}_2\text{O}_2$ process from 29.70 to 87.79% within 10 min . The investigation is consistent with previous studies which generally observed an increase in decolorization rate with increasing UV intensity (Mills et al., 1993; Lea and Adesina, 1998). This is a consequence of a higher quantity of generated $\bullet\text{OH}$ radicals, which make oxidative decolorization of anthraquinone dye more efficient.

The influence of UV light intensity on the decolorization of RB 19 by $\text{TiO}_2/\text{UV}/\text{KBrO}_3$ and $\text{TiO}_2/\text{UV}/(\text{NH}_4)_2\text{S}_2\text{O}_8$ processes has been monitored by varying the UV radiation intensity as in previous experiments, and similar results were obtained.

Comparison of decolorization by $\text{TiO}_2/\text{UV}/\text{KBrO}_3$, $\text{TiO}_2/\text{UV}/\text{H}_2\text{O}_2$ and $\text{TiO}_2/\text{UV}/(\text{NH}_4)_2\text{S}_2\text{O}_8$

In order to optimize the process, a comparison was made between the three heterogeneous oxidation processes after

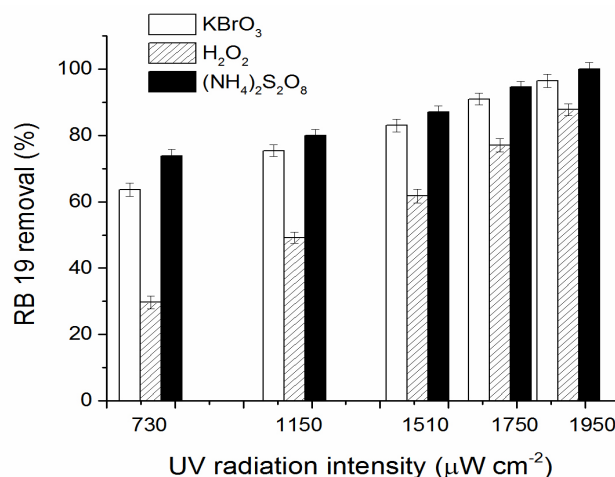


Figure 3. The removal efficiency of RB 19 by $\text{TiO}_2/\text{UV}/\text{KBrO}_3$, $\text{TiO}_2/\text{UV}/\text{H}_2\text{O}_2$ and $\text{TiO}_2/\text{UV}/(\text{NH}_4)_2\text{S}_2\text{O}_8$ processes as a function of radiation intensity. $[\text{RB19}]_0 = 50.0 \text{ mg}\cdot\text{dm}^{-3}$, $[\text{TiO}_2] = 1.0 \text{ g}\cdot\text{dm}^{-3}$, $[\text{KBrO}_3]_0 = 30.0 \text{ mmol}\cdot\text{dm}^{-3}$, $[\text{H}_2\text{O}_2]_0 = 30.0 \text{ mmol}\cdot\text{dm}^{-3}$, $[(\text{NH}_4)_2\text{S}_2\text{O}_8]_0 = 30.0 \text{ mmol}\cdot\text{dm}^{-3}$, initial pH 7.0 , temperature = $25.0 \pm 0.5^\circ\text{C}$.

10 min of treatment under given conditions. The initial electron acceptor concentrations in these experiments were 30.0 mmol·dm⁻³, and the amount of TiO₂ was 1.0 g·dm⁻³. In the case of photocatalytic decolorization, S₂O₈²⁻ is the most effective for the photodecolorization of RB 19 among the additives studied in this paper. The decolorization efficiencies of RB 19 are in the following order TiO₂/UV/(NH₄)₂S₂O₈ (100%) > TiO₂/UV/KBrO₃ (96.38%) > TiO₂/UV/H₂O₂ (87.79%).

Electron acceptors such as hydrogen peroxide, potassium bromate and ammonium persulfate were added into the solution in order to enhance the decolorization (Poulios and Tschpinis, 1999; Gratzel et al., 1990; Sanchez et al., 1998). All the additives showed a beneficial effect on the decolorization of the dye, whereas S₂O₈²⁻ has been found to remarkably enhance the decolorization of pollutant. The efficiency of the TiO₂/UV/H₂O₂ process is comparable to the TiO₂/UV/KBrO₃ process.

TiO₂-based photocatalysts also offer advantages such as high physical and chemical stability, low cost, availability, low toxicity, and excellent photoactivity (Banerjee et al., 2014). However, purification of water and wastewater using the TiO₂/UV/KBrO₃ process leads to the formation of bromide ions (Lv et al., 2008). Although bromide ion are not harmful to the human body, they can be converted to bromated and other brominated pollutants (Haag and Holgne, 1983; Gunten and Oliveras, 1998) which have suspected carcinogenic potential. Therefore, it is necessary and significant to remove the DBP (disinfection by-product) precursor bromide.

A traditional precursor removal strategy (enhanced coagulation) and novel precursor removal strategy (anion exchange such as activated carbon adsorption processes) are two areas of active research for controlling DBP formation (Johnson and Singer, 2004; Boyer and Singer, 2005). Also, Br⁻ ions are absorbed on the surface of TiO₂ and the ability to convert them into BrO₃⁻ ions is reduced. In the case of TiO₂/UV/H₂O₂, the final products of dyes degradation are carbon dioxide, water and inert salts (Muruganandham et al., 2004b; Sharma et al., 2016). The persulfates have high solubility and stability at ambient temperature, while the sulfate ions, which are the major products of persulfate reduction, are relatively harmless and considered to be environmentally friendly (Peternel et al., 2012; Olmez-Hanci et al., 2014). Therefore, these processes are a promising environmental engineering technique.

Effect of salt addition and decolorization test of RB 19 in surface water and dyebath effluent water

Starting from the assumption that the typical constituents of natural water and wastewater (CO₃²⁻, HCO₃⁻, SO₄²⁻, Cl⁻, NO₃⁻, HPO₄²⁻, H₂PO₄⁻) can influence the rate of decolorization of the tested substrates, the effects of different concentrations of some ions were studied. Decolorization experiments were performed by dissolving 50.0 mg·dm⁻³ of dye in deionized water. The added amount of catalyst was 1.0 g·dm⁻³ and the initial pH was 7.0. The obtained results are shown in Table 2.

The decrease in decolorization efficiency of the dye is due to the hole scavenging and hydroxyl radical scavenging properties of chloride and sulfate ions (Wei et al., 2009; Wenhua et al., 2000). The presence of bicarbonate increased the decolorization efficiency. Bicarbonate ions react with hydroxyl radical and produce carbonate radical, CO₃•⁻ (Aleboyeh et al., 2012). The carbonate radical is a strong oxidant and very selective for organic compounds.

In order to confirm the behaviour of RB 19 decolorization by TiO₂/UV/KBrO₃, TiO₂/UV/H₂O₂ and TiO₂/UV/(NH₄)₂S₂O₈ processes in different practical water samples under optimal

conditions, we chose three kinds of water samples as experimental matrices: (i) laboratory deionized water (DW) as the simulation wastewater treatment effluent, (ii) surface water (SW) collected from the Nišava River (pH 7.2, Ca⁺ = 79 mg·dm⁻³, Mg⁺ = 21 mg·dm⁻³, Na⁺ = 13.42 mg·dm⁻³, Cl⁻ = 69 mg·dm⁻³, SO₄²⁻ = 35 mg·dm⁻³, HCO₃⁻ = 240 mg·dm⁻³), and (iii) dyebath effluent water (DEW) collected from a local cotton dyeing facility. Dyebath effluent contained 0.050 g·dm⁻³ of dye RB 19. Assisting chemicals were also present in reactive dyebath effluent: 40 g·dm⁻³ NaCl (electrolyte, aggregation of dye onto fabric), 13 g·dm⁻³ Na₂CO₃ (pH buffer), 0.51 g·dm⁻³ NaOH (produces covalent bonds between dyestuff and fabric), 0.79 g·dm⁻³ nactic acid (neutralization), 0.50 g·dm⁻³ alkylphenol polyglycol ether (detergent, washing out of unfixed dyestuff). For preparing a model effluent, dyebath effluent wastewater was diluted to obtain a new solution with 50.0 mg·dm⁻³ of RB 19. RB 19 was spiked in surface water after the water sample's filtration, with initial concentration of 50 mg·dm⁻³. Figure 4 shows the removal efficiency of RB 19 obtained by TiO₂/UV/KBrO₃, TiO₂/UV/H₂O₂ and TiO₂/UV/(NH₄)₂S₂O₈ processes. Each process was carried out in all three matrices: DW, SW and DEW.

After 10 min irradiation, the TiO₂/UV/KBrO₃ process achieved 96.38%, 89.63% and 79.99% RB 19 removal for the DW, SW, and DEW, respectively; the TiO₂/UV/H₂O₂ process achieved 81.84%, 77.34% and 69.56% for the DW, SW, and DEW, respectively; and the TiO₂/UV/(NH₄)₂S₂O₈ process 100.0%, 96.56% and 86.35% for the DW, SW, and DEW, respectively. As shown in Fig. 4, in the surface water and dyebath effluent the efficiency of removal of RB 19 was lower than that achieved in the deionized water because of the interference of complex constituents in the surface water and dyebath effluent.

LS-MS analyses

On the mass spectra obtained after the applied heterogeneous oxidation processes, signals are observed at similar m/z values, so it can be assumed that the degradation of the RB 19 dye by the applied processes is probably carried out by a similar mechanism.

After the preliminary fragmentation of RB 19, the samples obtained during treatment with selected heterogeneous advanced oxidation processes were analysed. In Fig. 5b it can be seen from the mass spectrum of the sample after 2 min of treatment that a new ion at m/z of 499.1 was reported, compared to the spectrum of untreated dye sample. MS² ion analysis on m/z 499.1 gave ions on m/z 435.1 and m/z 408.0. These ions are found at m/z values greater than Δm/z 16 of the fragments at m/z 419.1 and 393.0 of the untreated RB 19 dye sample. Based on these facts, it can be assumed that the formation of mono-hydroxylated products has occurred.

Table 2. Effect of Cl⁻, SO₄²⁻ and HCO₃⁻ ions concentrations on the photodecolorization efficiency

Process	Conc. ion (mmol·dm ⁻³)	Decolorization (%)		
		Cl ⁻	SO ₄ ²⁻	HCO ₃ ⁻
TiO ₂ /UV/KBrO ₃	0	98.12	98.12	98.12
	10.0	89.39	87.92	100.0
	100.0	84.01	80.15	100.0
	1 000.0	77.55	70.38	100.0
TiO ₂ /UV/H ₂ O ₂	0	96.13	96.13	96.13
	10.0	87.40	94.42	100.0
	100.0	82.17	87.51	100.0
	1 000.0	75.14	77.19	100.0
TiO ₂ /UV/(NH ₄) ₂ S ₂ O ₈	0	100.0	100.0	100.0
	10.0	91.40	90.85	100.0
	100.0	87.15	82.64	100.0
	1 000.0	79.05	76.35	100.0

In the mass spectrum of the sample after 4 min of treatment, the peak intensity at m/z 602.9 was significantly reduced, and in the spectrum there was a peak at m/z 317.1 (Fig. 5c). The presence of this ion indicates one of the possible mechanisms of degradation where there is a breakdown of the relationship between the carbon of the aromatic nucleus and nitrogen. MS² fragmentation of the peak at m/z 317.1 gave an ion on m/z 253.2.

After 6 min of treatment, in the mass spectrum of the dye RB 19, no further signal is available on m/z 602.9 (Fig. 5 (d)). A new signal is an output at m/z 515.1. MS² analysis of the ion on m/z 515.1 gave a peak at m/z 451.1. The ion on m/z 451.1 is found at m/z values greater than $\Delta m/z$ 16 from ion to m/z 435.1 identified by the MS² analysis of the ion at m/z 499.1 after 2 min of colour treatment, which is probably due to the attachment of another •OH radical to an anthraquinone nucleus and the formation of a di-hydroxylated degradation product. MS³ ion analysis on m/z 451.1 gave ions on m/z 424.9, 377.2 and 360.2, while MS² ion analysis on m/z 499.1 obtained peaks at 435.1 and 408.1.

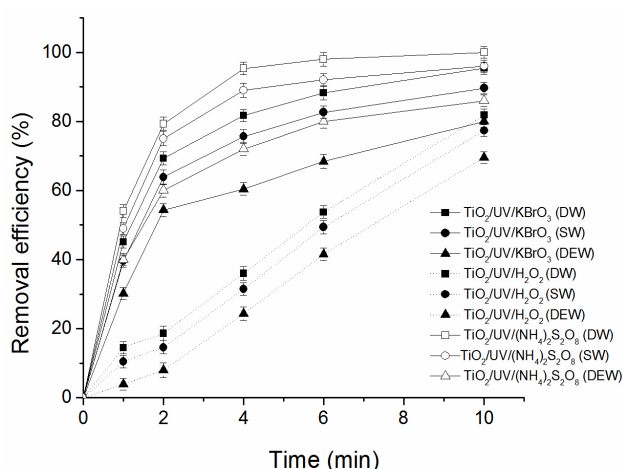


Figure 4. The removal of RB 19 by different oxidation processes: $\text{TiO}_2/\text{UV}/\text{KBrO}_3$ ($\text{pH} = 7.0$, $[\text{RB19}]_0 = 50.0 \text{ mg}\cdot\text{dm}^{-3}$, $\text{TiO}_2 = 1.0 \text{ g}\cdot\text{dm}^{-3}$, $[\text{KBrO}_3]_0 = 30.0 \text{ mmol}\cdot\text{dm}^{-3}$, UV intensity $1950 \mu\text{W}\cdot\text{cm}^{-2}$), $\text{TiO}_2/\text{UV}/\text{H}_2\text{O}_2$ ($\text{pH} = 7.0$, $[\text{RB19}]_0 = 50.0 \text{ mg}\cdot\text{dm}^{-3}$, $\text{TiO}_2 = 1.0 \text{ g}\cdot\text{dm}^{-3}$, $[\text{H}_2\text{O}_2]_0 = 30.0 \text{ mmol}\cdot\text{dm}^{-3}$, UV intensity $1950 \mu\text{W}\cdot\text{cm}^{-2}$) and $\text{TiO}_2/\text{UV}/(\text{NH}_4)_2\text{S}_2\text{O}_8$ ($\text{pH} = 7.0$, $[\text{RB19}]_0 = 50.0 \text{ mg}\cdot\text{dm}^{-3}$, $\text{TiO}_2 = 1.0 \text{ g}\cdot\text{dm}^{-3}$, $[(\text{NH}_4)_2\text{S}_2\text{O}_8]_0 = 30.0 \text{ mmol}\cdot\text{dm}^{-3}$, UV intensity $1950 \mu\text{W}\cdot\text{cm}^{-2}$)

After 10 min of treatment, no new signals were detected, and the intensities of all previously detected peaks were significantly reduced. After a longer treatment time (60 min), the signals of all detected ions have disappeared, indicating further oxidative degradation of intermediate products. Further degradation leads to the formation of low molecular weight aldehydes, organic acids, nitrate and sulfate that cannot be detected by this technique (Amorisco et al., 2011, 2013). These results are consistent with the results for the change in RB 19 dye concentration over time (Fig. 1), which show a significant drop in dye concentration at the same time. Based on the structure of the intermediate degradation products identified by the ESI/IT technique, a possible mechanism of degradation of the anthraquinone dye RB 19 can be predicted (Fig. 6).

CONCLUSIONS

The decolorization of the RB 19 solutions by $\text{TiO}_2/\text{UV}/\text{KBrO}_3$, $\text{TiO}_2/\text{UV}/\text{H}_2\text{O}_2$ and $\text{TiO}_2/\text{UV}/(\text{NH}_4)_2\text{S}_2\text{O}_8$ processes strongly depends on the system parameters, such as electron acceptors, dye initial concentration and radiation intensity. From an economic point of view, the $\text{TiO}_2/\text{UV}/(\text{NH}_4)_2\text{S}_2\text{O}_8$ process emerges as the most attractive oxidation system for reactive dye effluents in terms of complete decolorization (100.00% in less than 10 min), very closely followed by the $\text{TiO}_2/\text{UV}/\text{KBrO}_3$ process (96.44% after 10 min) and $\text{TiO}_2/\text{UV}/\text{H}_2\text{O}_2$ process (87.79% after 10 min). The presence of chloride and sulfate ions decreased the photocatalytic decolorization, while the presence of bicarbonate increased the decolorization efficiency. All three oxidation processes were carried out in three matrices (laboratory deionized water, surface water collected from the Nišava River and dyebath effluent water from a local cotton dyeing facility). In the surface water and dyebath effluent, the removal efficiency of RB 19 was lower than that achieved in the deionized water because of the interference of complex constituents in the surface water and the dyebath effluent. Lastly, LS-MS analyses were carried out to identify the intermediates produced during dye degradation. At longer treatment times no organic by-products were identified by LS-MS.

ACKNOWLEDGEMENTS

The authors would like to acknowledge financial support to the Ministry of Education, Science and Technological Development of the Republic of Serbia (Grant No TR34008).

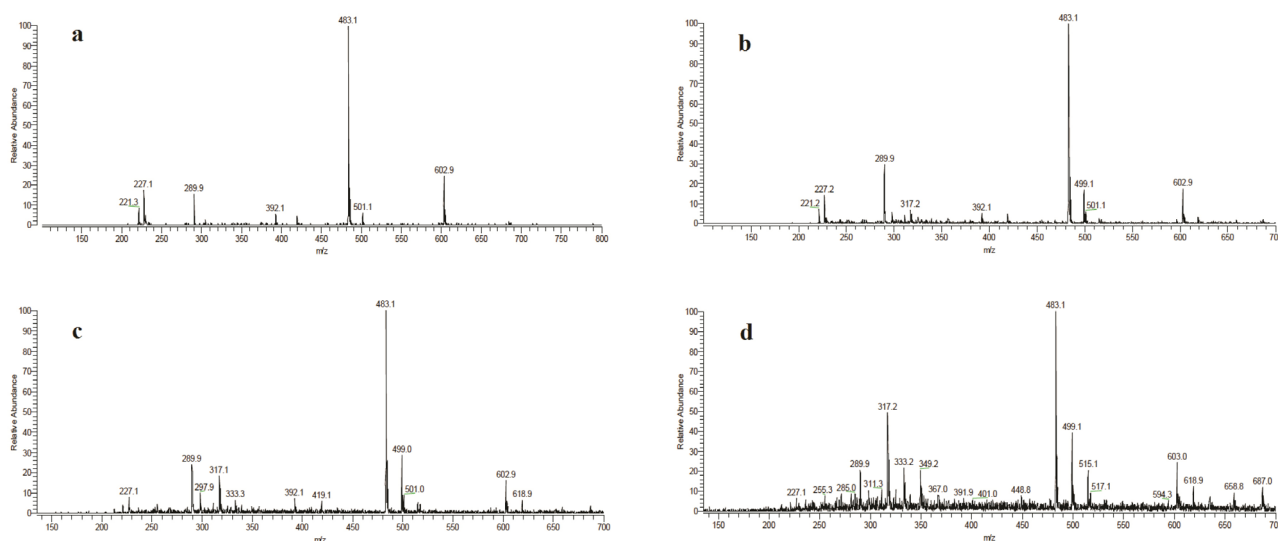


Figure 5. LC-MS spectra of the identified compound in RB 19 solution within 6 min of treatment: (a) RB 19 without treatment, (b) after 2 min (c) after 4 min (d) after 6 min

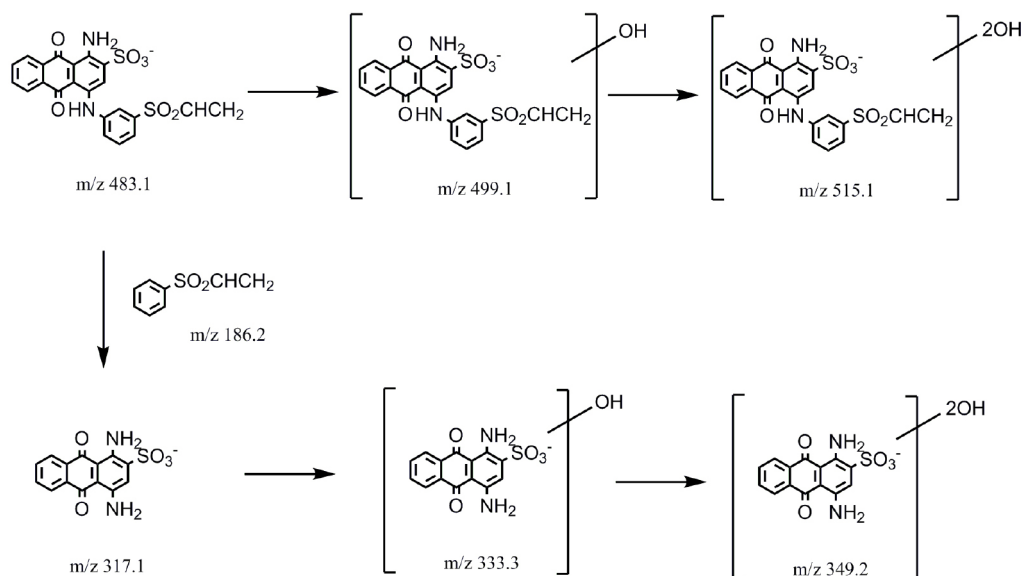


Figure 6. The proposed degradation pathways of RB 19

REFERENCES

- ALEBOYEH A, KASIRI MB and ALEBOYEH H (2012) Influence of dyeing auxiliaries on AB74 dye degradation by UV/H₂O₂ process. *J. Environ. Manage.* **113** 426–431. <https://doi.org/10.1016/j.jenvman.2012.10.008>
- ALEBOYEH A, MOUSSA Y and ALEBOYEH H (2005) The effect of operational parameters on UV/H₂O₂ decolourisation of Acid Blue 74. *Dyes Pigm.* **66** 129–134. <https://doi.org/10.1016/j.dyepig.2004.09.008>
- AMORISCO A, LOCAPUTO V and MASCOLO G (2011) Characterization of carbonyl by-products during Uniblu-A ozonation by liquid chromatography/hybrid quadrupole time-of-flight/mass spectrometry. *Rapid Commun. Mass Spectrom.* **25** (13) 1801–1811. <https://doi.org/10.1002/rcm.5045>
- AMORISCO A, LOCAPUTO V, PASTORE C and MASCOLO G (2013) Identification of low molecular weight organic acids by ion chromatography/hybrid quadrupole time-of-flight mass spectrometry during Uniblu-A ozonation. *Rapid Commun. Mass Spectrom.* **27** (1) 187–199. <https://doi.org/10.1002/rcm.6429>
- AYEDL, CHAIEB K, CHEREF A, BAKHROUF A (2010) Biodegradation and decolorization of triphenylmethane dyes by *Staphylococcus epidermidis*. *Desalination* **260** (1–3) 137–146. <https://doi.org/10.1016/j.desal.2010.04.052>
- BANERJEE S, PILLAI SC, FALARAS P, O'SHEA KE, BYRNE JA and DIONYSIOU DD (2014) New insights into the mechanism of visible light photocatalysis. *J. Phys. Chem. Lett.* **5** (15) 2543–2554. <http://dx.doi.org/10.1021/jz501030x>
- BEHNAJADY MA, MODIRSHAHLA N and SHOKRI M (2004) Photodestruction of Acid Orange 7 (AO7) in aqueous solutions by UV/H₂O₂: influence of operational parameters. *Chemosphere* **55** (1) 129–134. <https://doi.org/10.1016/j.chemosphere.2003.10.054>
- BOYER TH and SINGER PC (2005) Bench-scale testing of a magnetic ion exchange resin for removal of disinfection by-product precursors. *Water Res.* **39** (7) 1265–1276. <https://doi.org/10.1016/j.watres.2005.01.002>
- BRILLAS E, CALPE JC and CASADO J (2000) Mineralization of 2,4-D by advanced electrochemical oxidation processes. *Water Res.* **34** (8) 2253–2262. [https://doi.org/10.1016/S0043-1354\(99\)00396-6](https://doi.org/10.1016/S0043-1354(99)00396-6)
- CETINKAYA T, NEUWIRTHOVA L, KUTLAKOVA KM, TOMASEK V and AKBULUT H (2013) Synthesis of nanostructured TiO₂/SiO₂ as an effective photocatalyst for degradation of acid orange. *Appl. Surf. Sci.* **279** 384–390. <https://doi.org/10.1016/j.apsusc.2013.04.121>
- CHEN F, HE J, ZHAO J and YU JC (2002) Photo-Fenton degradation of Malachite Green catalyzed by aromatic compounds under visible light irradiation. *New J. Chem.* **26** (3) 336–341. <http://dx.doi.org/10.1039/B107404K>
- CHEN SF and LIU YZ (2007) Study on the photocatalytic degradation of glyphosate by TiO₂ photocatalyst. *Chemosphere* **67** (5) 1010–1017. <https://doi.org/10.1016/j.chemosphere.2006.10.054>
- CHEN YP, LIU SY, YU HQ, YIN H and LI QR (2008) Radiation-induced degradation of methyl orange in aqueous solutions. *Chemosphere* **72** (4) 532–536. <https://doi.org/10.1016/j.chemosphere.2008.03.054>
- CHU W and WONG CC (2004) The photocatalytic degradation of dicamba in TiO₂ suspensions with the help of hydrogen peroxide by different near UV irradiations. *Water Res.* **38** (4) 1037–1043. <https://doi.org/10.1016/j.watres.2003.10.037>
- DANESHVAR N and KHATAEE AR (2006) Removal of azo dye C.I. Acid Red 14 from contaminated water using Fenton, UV/H₂O₂, UV/H₂O₂/Fe(II), UV/H₂O₂/Fe(III), and UV/H₂O₂/Fe(III)/oxalate processes: a comparative study. *J. Environ. Sci. Health A* **41** (3) 315–328. <https://doi.org/10.1080/10934520500423196>
- DANESHVAR N, SALARI D and KHATAEE AR (2003) Photocatalytic degradation of azo dye Acid Red 14 in water: investigation of the effect of operational parameters. *J. Photochem. Photobiol. A* **157** (1) 111–116. [https://doi.org/10.1016/S1010-6030\(03\)00015-7](https://doi.org/10.1016/S1010-6030(03)00015-7)
- DANESHVAR N, SALARI D, NIAIE A, RASOULIFARD MH and KHATAEE AR (2005a) Immobilization of TiO₂ nanopowder on glass beads for the photocatalytic decolorization of an azo dye C.I. Direct Red 23. *J. Environ. Sci. Health A* **40** (8) 1605–1617. <https://doi.org/10.1081/ESE-200060664>
- DANESHVAR N, RABBANI M, MODIRSHAHLA N and BEHNAJADY MA (2005b) Photooxidative degradation of Acid Red 27 in tubular continuous-flow photoreactor: influence of operational parameters and mineralization products. *J. Hazardous Mater. B* **118** (1–3) 155–160. <https://doi.org/10.1016/j.jhazmat.2004.10.007>
- DANESHVAR N, KHATAEE AR, RASOULIFARD MH and HOSSEINZADEH E (2007) Removal of C.I. Acid Orange 7 from aqueous solution by UV irradiation in the presence of ZnO nanopowder. *J. Hazardous Mater.* **143** (1–2) 95–101. <https://doi.org/10.1016/j.jhazmat.2006.08.072>
- DIONYSIOU DD, SUIDAN MT, BEKOU E, BAUDIN I and LAINE JM (2000) Effect of ionic strength and hydrogen peroxide on the photocatalytic degradation of 4-chlorobenzoic acid in water. *Appl. Catal. B: Environ.* **26** (3) 153–171. [https://doi.org/10.1016/S0926-3373\(00\)00124-7](https://doi.org/10.1016/S0926-3373(00)00124-7)
- ELMORSI TM, RIYAD YM, MOHAMED ZH, ABD EL BARY HMH (2010) Decolorization of Mordant red 73 azo dye in water using H₂O₂/UV and photo-Fenton treatment. *J. Hazardous Mater.* **174** (1–3) 352–358. <https://doi.org/10.1016/j.jhazmat.2009.09.057>
- FLOX C., AMMAR S, ARIAS C, BRILLAS E, VARGAS-ZAVALA AV and ABDEIHEDI R (2006) Electro-Fenton and photoelectron-Fenton degradation of indigo carmine in acidic aqueous medium. *Appl. Catal. B* **67** (1–2) 93–104. <https://doi.org/10.1016/j.apcatb.2006.04.020>
- FOX MA and DULAY MT (1993) Heterogeneous photocatalysis. *Chem. Rev.* **93** (1) 341–357. <https://doi.org/10.1021/cr00017a016>
- FUJISHIMA A, RAO TN and TRYK DA (2000) Titanium dioxide

- photocatalysis. *J. Photochem. Photobiol. C* **1** (1) 1–21. [https://doi.org/10.1016/S1389-5567\(00\)00002-2](https://doi.org/10.1016/S1389-5567(00)00002-2)
- GALINDO C and KALT A (1998) UV–H₂O₂ oxidation of monoazo dyes in aqueous media: a kinetic study. *Dyes Pigm.* **40** (1) 27–35. [https://doi.org/10.1016/S0143-7208\(98\)00027-8](https://doi.org/10.1016/S0143-7208(98)00027-8)
- GANESH R, BOARDMAN GD and MICHELSON D (1994) Fate of azo dyes in sludges. *Water Res.* **28** (6) 1367–1376. [https://doi.org/10.1016/0043-1354\(94\)90303-4](https://doi.org/10.1016/0043-1354(94)90303-4)
- GHODBANE H and HAMDAOUI O (2010) Decolorization of anthraquinonic dye C.I. Acid Blue 25, in aqueous solution by direct UV irradiation, UV/H₂O₂ and UV/Fe(II) processes. *Chem. Eng. J.* **160** (1) 226–231. <https://doi.org/10.1016/j.cej.2010.03.049>
- GRATZEL, CK, JIROUSEK M and GRATZEL M (1990) Decomposition of organophosphorus compounds on photoactivated TiO₂ surfaces. *J. Mol. Catal.* **60** (3) 375–387. [https://doi.org/10.1016/0304-5102\(90\)85260-O](https://doi.org/10.1016/0304-5102(90)85260-O)
- GUNTEN U and OLIVERAS Y (1998) Advanced oxidation of bromide-containing waters: bromated formation mechanisms. *Environ. Sci. Technol.* **32** (1) 63–70. <https://doi.org/10.1021/es970477j>
- HAAG WR and HOLGNE J (1983) Ozonation of bromide-containing waters: kinetics of formation of hypobromous acid and bromate. *Environ. Sci. Technol.* **17** (5) 261–267. <https://doi.org/10.1021/es00111a004>
- HOLKAR CR, JADHAV AJ, PINJARI DV, MAHAMUNI NM and PANDIT AB (2016) A critical review on textile wastewater treatments: possible approaches. *J. Environ. Manage.* **182** 351–366. <https://doi.org/10.1016/j.jenvman.2016.07.090>
- HOSSAIN L, SARKER SK and KHAN MS (2018) Evaluation of present and future wastewater impacts of textile dyeing industries in Bangladesh. *Environ. Dev.* **26** 23–33. <https://doi.org/10.1016/j.envdev.2018.03.005>
- HOUAS A, LACHHEB H, KSIBI M, ELALOUI E, GUILLARD C and HERRMANN JM (2001) Photocatalytic degradation pathway of methylene blue in water. *Appl. Catal. B: Environ.* **31** (2) 145–157. [https://doi.org/10.1016/S0926-3373\(00\)00276-9](https://doi.org/10.1016/S0926-3373(00)00276-9)
- JOHNSON CJ and SINGER PC (2004) Impact of a magnetic ion exchange resin on ozone demand and bromated formation during drinking water treatment. *Water Res.* **38** (17) 3738–3750. <https://doi.org/10.1016/j.watres.2004.06.021>
- LEA J and ADESINA AA (1998) The photo-oxidative degradation of sodium dodecyl sulfate in aerated aqueous TiO₂ suspension. *J. Photochem. Photobiol. A* **118** (2) 111–122. [https://doi.org/10.1016/S1010-6030\(98\)00375-X](https://doi.org/10.1016/S1010-6030(98)00375-X)
- LEDKOWICZ S, SOLECKA M and ZYLLA R (2001) Biodegradation, decolourisation and detoxification of textile wastewater enhanced by advanced oxidation processes. *J. Biotechnol.* **89** (2–3) 175–184. [https://doi.org/10.1016/S0168-1656\(01\)00296-6](https://doi.org/10.1016/S0168-1656(01)00296-6)
- LI W and WU H (2017) Sodium citrate functionalized reusable Fe₃O₄@TiO₂ photocatalyst for water purification. *Chem. Phys. Lett.* **686** 178–182. <https://doi.org/10.1016/j.cplett.2017.08.046>
- LINSEBIGLER AL, LU GQ and YATES JT (1995) Photocatalysis on TiO₂ Surfaces: Principles, Mechanisms, and Selected Results. *Chem. Rev.* **95** (4) 735–758. <https://doi.org/10.1021/cr00035a013>
- LV L, WANG Y, WEI M and CHENG J (2008) Bromide ion removal from contaminated water by calcined and uncalcined MgAl-CO₃ layered double hydroxides. *J. Hazardous Mater.* **152** (3) 1130–1137. <https://doi.org/10.1016/j.jhazmat.2007.07.117>
- MASUM M (2016) The Bangladesh textile-clothing industry: a demand-supply review. *Social Syst. Stud.* **9** 109–139.
- MIGUEL R, VICTOR S, SANTIAGO E and CESAR P (2002) Photo-Fenton treatment of a bio-recalcitrant wastewater generated in textile activities: biodegradability of the phototreated solution. *J. Photochem. Photobiol. A: Chem.* **151** (1–3) 129–135. [https://doi.org/10.1016/S1010-6030\(02\)00148-X](https://doi.org/10.1016/S1010-6030(02)00148-X)
- MILLS A, DAVIS R and WORSLEY D (1993) Water purification by semiconductor photocatalysis. *Chem. Soc. Rev.* **22** (6) 417–434. <https://doi.org/10.1039/CS9932200417>
- MITROVIC J, RADOVIC M, BOJIC D, ANDJELKOVIC T, PURENOVIC M and BOJIC A (2012) Decolorization of textile azo dye Reactive Orange 16 with UV/H₂O₂ process. *J. Serb. Chem. Soc.* **77** (4) 465–481. <https://doi.org/10.2298/JSCI10216187M>
- MOHEJ EL-DEIN A, LIBRA JA and WIESMANN U (2003). Mechanism and kinetic model for the decolorization of the azo dye Reactive Black 5 by hydrogen peroxide and UV radiation. *Chemosphere* **52** (6) 1069–1077. [https://doi.org/10.1016/S0045-6535\(03\)00226-1](https://doi.org/10.1016/S0045-6535(03)00226-1)
- MUNEERA M and BAHNEMANN D (2002) Semiconductor-mediated photocatalyzed degradation of two selected pesticide derivatives, terbacil and 2,4,5-tribromimidazole, in aqueous suspension. *Appl. Catal. B: Environ.* **36** (2) 95–111. [https://doi.org/10.1016/S0926-3373\(01\)00282-X](https://doi.org/10.1016/S0926-3373(01)00282-X)
- MURUGANANDHAM M and SWAMINATHAN M (2004a) Decolourisation of Reactive Orange 4 by Fenton and photo-Fenton oxidation technology. *Dyes Pigm.* **63** (3) 315–321. <https://doi.org/10.1016/j.dyepig.2004.03.004>
- MURUGANANDHAM M and SWAMINATHAN M (2004b) Photochemical oxidation of reactive azo dye with UV–H₂O₂ process. *Dyes Pigm.* **62** (3) 269–275. <https://doi.org/10.1016/j.dyepig.2003.12.006>
- OLMEZ-HANCI T, ARSLAN-ALATON I and GENC B (2014) Degradation of the nonionic surfactant Triton™ X-45 with HO• and SO₄•– based advanced oxidation processes. *Chem. Eng. J.* **239** 332–340. <https://doi.org/10.1016/j.cej.2013.11.033>
- PETERNEL I, KUSIC H, MARIN V and KOPRIVANAC N (2012) UV-assisted persulfate oxidation : the influence of cation type in persulfate salt on the degradation kinetic of azo dye pollutant. *React. Kinet. Mech. Catal.* **108** (1) 17–39. <http://dx.doi.org/10.1007/s11144-012-0502-9>
- PICHA T, GUILLARD C, AMALRIC L, RENARD A and PLAIDY O (1995) Assessment of the importance of the role of H₂O₂ and O₂•– in the photocatalytic degradation of 1,2-dimethoxybenzene. *Sol. Energy Mater. Sol. Cells* **38** (1–4) 391–399. [https://doi.org/10.1016/0927-0248\(94\)00231-2](https://doi.org/10.1016/0927-0248(94)00231-2)
- PIERA E, CALPE JC, BRILLAS E, DOMENECH X and PERAL J (2000) 2,4-Dichlorophenoxyacetic acid degradation by catalyzed ozonation: TiO₂/UVA/O₃ and Fe(II)/UVA/O₃ systems. *Appl. Catal. B.* **27** (3) 169–177. [https://doi.org/10.1016/S0926-3373\(00\)00149-1](https://doi.org/10.1016/S0926-3373(00)00149-1)
- POULIOS I and TSACHPINIS I (1999) Photodegradation of the textile dye Reactive Black 5 in the presence of semiconducting oxides. *J. Chem. Technol. Biotechnol.* **74** (4) 349–357. [http://dx.doi.org/10.1002/\(SICI\)1097-4660\(199904\)74:4%3C349::AID-JCTB5%3E3.0.CO;2-7](http://dx.doi.org/10.1002/(SICI)1097-4660(199904)74:4%3C349::AID-JCTB5%3E3.0.CO;2-7)
- PUNZI M, NILSSON F, ANBALAGAN A, SVENSSON BM, JONSSON K, MATTIASSON B and JONSTRUP M (2015) Combined anaerobic-ozonation process for treatment of textile wastewater: removal of acute toxicity and mutagenicity. *J. Hazardous Mater.* **292** 52–60. <https://doi.org/10.1016/j.jhazmat.2015.03.018>
- RAUF MA, MEETANI MA, KHALEEL A and AHMED A (2010) Photocatalytic degradation of Methylene Blue using a mixed catalyst and product analysis by LC/MS. *Chem. Eng. J.* **157** (2–3) 373–378. <https://doi.org/10.1016/j.cej.2009.11.017>
- RIBEIRO MCM, STARLING MCM, LEAO MMD and DE AMORIM CC (2017) Textile wastewater reuse after additional treatment by Fenton's reagent. *Environ. Sci. Pollut. Res.* **24** (7) 6165–6175. <https://doi.org/10.1007/s11356-016-6921-9>
- ROSENFELDT EJ, LINDEN KG, CANONICA S and VON GUNTEN U (2006) Comparison of the efficiency of •OH radical formation during ozonation and the advanced oxidation processes O₃/H₂O₂ and UV/H₂O₂. *Water Res.* **40** (20) 3695–3704. <https://doi.org/10.1016/j.watres.2006.09.008>
- SAN N, HATIPOGLU A, KOCTURK G and CINAR Z (2001) Prediction of primary intermediates and the photodegradation kinetics of 3-aminophenol in aqueous TiO₂ suspensions. *J. Photochem. Photobiol. A: Chem.* **139** (2–3) 225–232. [https://doi.org/10.1016/S1010-6030\(01\)00368-9](https://doi.org/10.1016/S1010-6030(01)00368-9)
- SANCHEZ L, PERAL J and DOMENECH X (1998) Aniline degradation by combined photocatalysis and ozonation. *Appl. Cat. B Environ.* **19** (1) 59–65. [https://doi.org/10.1016/S0926-3373\(98\)00058-7](https://doi.org/10.1016/S0926-3373(98)00058-7)
- SHARMA J, MISHRA IM and KUMAR V (2016) Mechanistic study of photo-oxidation of Bisphenol-A (BPA) with hydrogen peroxide (H₂O₂) and sodium persulfate (SPS). *J. Environ. Manage.* **166** (15) 12–22. <https://doi.org/10.1016/j.jenvman.2015.09.043>
- SHAROTRI N and SUD D (2017) Visible light responsive Mn-S-co-doped TiO₂ photocatalyst – Synthesis, characterization and mechanistic aspect of photocatalytic degradation. *Sep. Purif. Technol.* **183** 382–391. <https://doi.org/10.1016/j.seppur.2017.03.053>
- SHU HY and CHANG MC (2005) Decolorization effect of six azo dyes by O₃, UV/O₃ and UV/H₂O₂ processes. *Dyes Pigm.* **65** (1) 25–31.

- <https://doi.org/10.1016/j.dyepig.2004.06.014>
- SO M, CHENG MY, YU JC and WONG PK (2002) Degradation of azo dye procion Red MX-5B by photocatalytic oxidation. *Chemosphere* **46** (6) 905–912. [https://doi.org/10.1016/S0045-6535\(01\)00153-9](https://doi.org/10.1016/S0045-6535(01)00153-9)
- SUBRAMANIAN V, WOLF E and KAMAT PV (2001) Semiconductor–metal composite nanostructures. to what extent do metal nanoparticles improve the photocatalytic activity of TiO₂ films? *J. Phys. Chem. B* **105** (46) 11439–11446. <https://doi.org/10.1021/jp011118k>
- TEHRANI-BAGHA AR, MAHMOODI NM and MENER FM (2010) Degradation of a persistent organic dye from colored textile wastewater by ozonation. *Desalination* **260** (1–3) 34–38. <https://doi.org/10.1016/j.desal.2010.05.004>
- VESELY M, CEPPAN M and LAPCIK L (1991) Photocatalytic degradation of hydroxyethylcellulose in aqueous Pt–TiO₂ suspension. *J. Photochem. Photobiol. A: Chem.* **61** (3) 399–406. [https://doi.org/10.1016/1010-6030\(91\)90023-M](https://doi.org/10.1016/1010-6030(91)90023-M)
- WAN Y, SUN B, XU Z and CHAO W (2012) Effect of UV irradiation on wear protection of TiO₂ and Ni-doped TiO₂ coatings. *Appl. Surf. Sci.* **258** (10) 4347–4350. <https://doi.org/10.1016/j.apsusc.2011.12.111>
- WANG W, HUANG WJ, NI Y, LU CH, TAN LJ and XU ZZ (2013) Graphene supported β NaYF₄:Yb³⁺, Tm³⁺ and N doped P25 nanocomposite as an advanced NIR and sunlight driven upconversion photocatalyst. *Appl. Surf. Sci.* **282** 832–837. <https://doi.org/10.1016/j.apsusc.2013.06.066>
- WANG X, YAO Z, WANG J, GUO W and LI G (2008) Degradation of reactive brilliant red in aqueous solution by ultrasonic cavitation. *Ultrason. Sonochem.* **15** (1) 43–48. <https://doi.org/10.1016/j.ultsonch.2007.01.008>
- WEBER EJ and ADAMS RL (1995) Chemical and sediment mediated reduction of the azo dye disperse blue 79. *Environ. Sci. Technol.* **29** (5) 1163–1170. <https://doi.org/10.1021/es00005a005>
- WEI L, SHIFU C, WEI Z and SUJUAN Z (2009) Titanium dioxide mediated photocatalytic degradation of methamidophos in aqueous phase. *J. Hazardous Mater.* **164** (1) 154–160. <https://doi.org/10.1016/j.jhazmat.2008.07.140>
- WENHUA L, HONG L, SUO'AN C, JIANQING Z and CHUNAN C (2000) Kinetics of photocatalytic degradation of aniline in water over TiO₂ supported on porous nickel. *J. Photochem. Photobiol. A: Chem.* **131** (1–3) 125–132. [https://doi.org/10.1016/S1010-6030\(99\)00232-4](https://doi.org/10.1016/S1010-6030(99)00232-4)
- XU GR, WANG JN and LI CJ (2013) Template directed preparation of TiO₂ nanomaterials with tunable morphologies and their photocatalytic activity research. *Appl. Surf. Sci.* **279** 103–108. <https://doi.org/10.1016/j.apsusc.2013.04.043>
- YANG MQ, ZHANG N and XU YJ (2013) Synthesis of fullerene-, carbon nanotube-, and graphene-TiO₂ nanocomposite photocatalysts for selective oxidation: a comparative study. *ACS Appl. Mater. Interfaces* **5** (3) 1156–1164. <https://doi.org/10.1021/am3029798>
- ZHANG F, ZHAO J, SHEN T, HIDAKA H, PELIZZETTI E and SERPONE N (1998) TiO₂-assisted photodegradation of dye pollutants II. Adsorption and degradation kinetics of eosin in TiO₂ dispersions under visible light irradiation. *Appl. Catal. B* **15** (1–2) 147–156. [https://doi.org/10.1016/S0926-3373\(97\)00043-X](https://doi.org/10.1016/S0926-3373(97)00043-X)
- ZHU G, QUE W and ZHANG J (2011) Synthesis and photocatalytic performance of Ag-loaded β -Bi₂O₃ microspheres under visible light irradiation. *J. Alloys Compd.* **509** (39) 9479–9486. <https://doi.org/10.1016/j.jallcom.2011.07.046>